

2nd CIRP Global Web Conference

Innovative Drive Concept for Machining Robots

Denkena, B.^a, Litwinski, K.^a, Schönherr, M.^{a*}

^aInstitute of Production Technology and Machine Tools, Leibniz Universität Hannover, An der Universität 2, 30823 Garbsen, Germany

* Corresponding author. Tel.: +49 511 762 18309; fax: +49 511 762 5115. E-mail address: schoenherr@ifw.uni-hannover.de.

Abstract

In this paper an innovative drive concept for robots to improve their machining capability is presented. As a test bed a two-axis robot is designed and equipped with torque motors with load-sided high resolution encoders in addition to conventional gear motors with harmonic drive gearboxes. The gear motors are used for positioning tasks while the torque motors in particular compensate static and dynamic load-sided angle errors. The model-based control algorithm is decoupled and separately actuates both the servo gear and torque motors. It is shown that a considerable increase of performance is possible when adding the torque motors especially regarding the compensation of dynamic angle errors. The paper will present the design and details of the new drive concept, the modeling basics and first simulation results.

© 2013 The Authors. Published by Elsevier B.V. Open access under [CC BY-NC-ND license](#).

Selection and peer-review under responsibility of International Scientific Committee of the 2nd CIRP Global Web Conference in the person of the Conference Chair Dr. Sotiris Makris

Keywords: Robotics; Machining; Design, Control Loop, Drive Chain

1. Introduction

Modern manufacturing enterprises are progressively dependent on increasing both flexibility and cost-effectiveness of machining processes e.g. by enhancing the automation of the processes or the process chains [1]. However, this requirement is opposed by high acquisition costs for automation systems and more flexible high performance machine tools [2]. State of the art machine tools are highly optimized for various manufacturing purposes and thus provide single-digit μm accuracy and high damping. In contrast, industrial robots provide high flexibility, low costs of purchase, a better ratio of work to installation space and they can be adopted for a wide application range [3]. But the application of robots for machining purposes is associated with significant disadvantages resulting in rare application of robots in material removal processes. Compared to state of the art machine tools they offer only low repeat and path accuracy as well as a very low position dependent stiffness. E.g. process forces at the tool center point of a spindle at the robot end-effector result in comparatively high deviations of the tool [4, 5]. Additionally they tend to low frequency structural vibrations due to dynamic

process force excitation [6]. These are the main reasons why the application of robots in the range of machining purposes is increasing but still less than 5% of the overall robotic sales [7]. Actual machining applications include for instance the pre-machining of castings or processes with low tolerances.

2. Innovative Hybrid Drive Concept

2.1. Motivation

Machining processes performed with industrial robots of the state of the art is considerably constricted as a consequence of significant both structural and control limitations. On the one hand the high compliance of the robot structure, as a consequence of the gear boxes and bearings in the robot joints [8, 9], leads to very low structural eigenfrequencies. Processing forces e.g. of a spindle at the robot end-effector thus cause both static deviations of the TCP (resulting from the gear box compliances) and structural vibrations. Both significantly affect the machining result in a negative manner. On the other hand limitations regarding the control environment restrict the control quality. Robot controls generally have single axis control implemented using the drive-sided

angular measurement systems of the drive motors. In addition usually component nonlinearities, e.g. backlash, friction, torque dependent stiffness of gear boxes, robot link deformation, etc. are neglected. Additionally the dynamic coupling between the separate axes due to centrifugal and Coriolis forces are disregarded whereby consequently a compensation of high dynamic positioning errors cannot be realized with this control concept. Apart from that a high dynamic compensation would fail due to the low pass characteristic of the gear box. Furthermore, the real load-sided joint angles cannot be detected by reason of missing direct measurements. Eventually low cycle times between controller and robot hardware prohibits real time compensation of angle errors at higher frequencies due to external excitations.

TCP	tool center point
LQR	linear quadratic regulator
\mathbf{q}	vector of joint angles
\mathbf{q}_M	vector of drawn gear motor angles
τ_{SM}	vector of gear motor torques
τ_{TM}	vector of torque motor torques
M	inertia matrix of robot
$\mathbf{g}(\mathbf{q})$	vector of gravity corresponding joint torques
$\mathbf{c}(\mathbf{q}, \dot{\mathbf{q}})$	vector of joint torques regarding centrifugal and Coriolis effects
K	diagonal matrix of gear box stiffness
K_E	matrix depending on K (cf. eq. (7))
F_{VSM}	vector of drive-sided viscous friction
F_{SSM}	vector of drive-sided static friction
F_V	vector of load-sided viscous friction
F_s	vector of load-sided static friction
K_R	control matrix
R	control energy weighting matrix for LQR
Q	state variables weighting matrix for LQR
P	solution of Matrix-Riccati-Equation

2.2. Hybrid drive concept

One approach for handling especially the structural insufficiencies is the exclusive application of direct drive [10, 11]. Thus, it enables the direct measurement of the real joint angle with the necessary encoder. Additionally, the control bandwidth of a joint drive chain extends leading to higher jerks, accelerations and velocities. However, the abdication of a gear box necessitates the compensation of load torques only with corresponding drives, thus leading to considerably higher energy consumption and hence increased operating costs.

The suggested innovative hybrid drive concept for robot joints is based on a direct coupling of the drive shafts of a conventional servo motor with a gear box and a torque motor, thus taking advantage of both motor types. This combination corresponds to a parallel connection of these motors. Additionally, the load-sided joint angle is measured with a high-resolution encoder.

Measuring the real load-side joint angles enables to directly compensate for angle errors resulting from the joint insufficiencies and thus to calculate the end-effector position with considerably more precision. The function of the integrated gear motor primarily is moving the robot along determined trajectories. The torque motors task with the load-sided encoder is in particular the static and dynamic compensation of angle errors induced by both the joint compliances and external forces and torques respectively. An increase of the dynamic stiffness as well as damping is anticipated.

As a result of this hybrid approach the advantages of the separate motor types are combined. The gear motor provides high torques with comparatively low energy consumption for positioning tasks and the torque motor offers a high bandwidth for high dynamic control influence. Furthermore, both motors can be planned with smaller sizes, because both motor torques are combined.

Compared to a holistic directly driven robot the suggested hybrid drive concept provides cost advantages regarding acquisition and maintenance. However, both the design complexity of the joint and the cost compared to a state of the art robot are increasing. Additionally a model based control of this drive concept features a more complex nonlinear character resulting in increasing computational resources.

2.3. Design of a two-axis test bed

To investigate the introduced hybrid drive concept a two axis test bed is designed (Fig. 1). It is planned to include both the gear and the torque motor in a preferably compact manner. Therefore, a double hollow shaft design is chosen. Thus, both motors are connected to apply the respective torque to the drive shaft. The gear motor has an integrated multi-turn absolute encoder for drive-sided angle measurement. The load-sided encoder is connected to both the drive-sided fixed link and the remotest position of the load-sided moveable link. Both motors are included in round pipe profile housings. This design is based on a preliminarily performed topology optimization of the link geometry. The link components are welded assemblies made of profiles. Thereby, the designed robot is structurally comparable to standard industrial robots with cast links. In order to realize a compact design a combined axial-radial bearing is chosen as commonly used for industrial robots. Compared to a design with at least two separate bearings this provides both a considerably more compact design and axial as well as tilting stiffness are comparable to standard industrial robots.

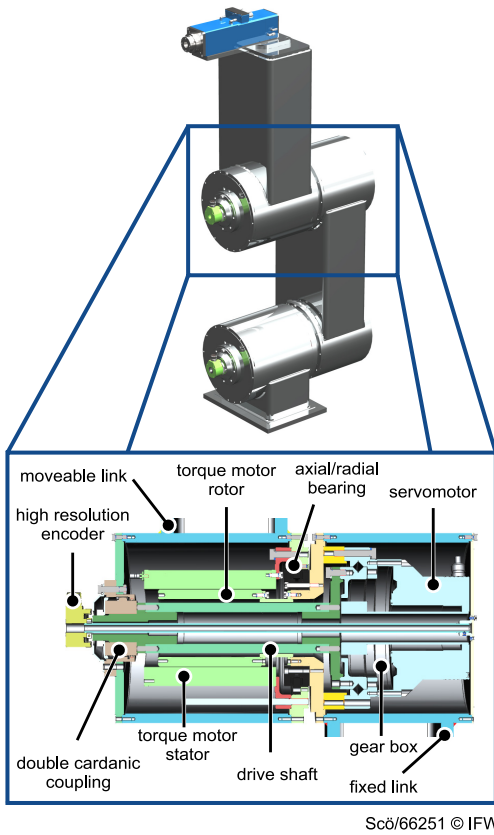


Fig. 1: Two-axis robot test bed with innovative hybrid drive concept: design and joint cross sectional view

Table 1: Selected drive components

Motor type	Manufacturer	Max. torque [Nm]	Max. speed [rpm]
gear motor	Harmonic Drive	1480	38
torque motor	Siemens	339	180
Bearing			
YRT120	INA	c _a	c _r
		2100	2200
			7000

The load-sided sin-cos-encoder with HIPERFACE interface provides a resolution of 2.5'' and thus an accuracy of approximately 12 μm per meter lever arm. Hence, compared to approximately 100 μm of state of the art industrial robots a considerable increase of positioning and path accuracy is anticipated.

3. Modeling of the Robot

3.1. Rigid body model

To analyze a robot motion a dynamic model is necessary to obtain information concerning required forces and torques and thus a basis for designing drives,

actuators and joints. In this paper the dynamic model is based on a Lagrange formulation method. Compared to the Newton-Euler formulation it is more conceptual, systematic and yields a compact analytical form containing the inertia matrix, centrifugal and Coriolis related and gravity related terms respectively. Additionally, it is advantageous for both control design and expanding it by more complex mechanical effects (e.g. friction, backlash, flexible link deformation, etc.).

Using the generalized forces τ and the generalized coordinates q Lagranges equation with Lagrangian L being the sum of T kinetic and U potential energy is the following.

$$\frac{d}{dt} \frac{\partial L}{\partial \dot{q}} - \frac{\partial L}{\partial q} = \tau \quad (1)$$

In this case τ represents the joint torques and q the joint angles. According to [12] the kinetic energy T consists of a translational and a rotational part.

$$T = \frac{1}{2} \sum_{i=1}^n (m_i \cdot {}^{(0)}\dot{r}_{S_i}^T \cdot {}^{(0)}\dot{r}_{S_i} + {}^{(0)}\omega_i^T \cdot {}^{(S_i)}I_i \cdot {}^{(0)}\omega_i) \quad (2)$$

The translational kinetic energy is represented by a mass m_i and the linear velocity of the center of this mass ${}^{(0)}\dot{r}_{S_i}$. The rotational kinetic energy can be calculated using the inertia tensor ${}^{(S_i)}I_i$ and the angular velocity ${}^{(0)}\omega_i$ of the respective body. Concerning the calculation of the kinetic energy of a robot it is relevant to consider both the robot links and the drive motors. In dependency of the general calculation of the kinetic energy the inertia matrix can be calculated using eq. (3)

$$M(q) = \sum_{i=1}^n (m_i \cdot {}^{(0)}J_{t_i}^T \cdot {}^{(0)}J_{t_i} + {}^{(0)}J_{r_i}^T \cdot {}^{(0)}I_i \cdot {}^{(0)}J_{r_i}) \quad (3)$$

with the translational Jacobi matrix ${}^{(0)}J_{t_i}$ and the rotational Jacobi matrix ${}^{(0)}J_{r_i}$. With the gravity acceleration vector g_0 and the partial derivative of the potential energy U concerning the generalized coordinates leads to the gravity related joint torques.

$$g(q) = - \sum_{j=1}^n m_j \cdot {}^{(0)}g_0^T \cdot J_{t_i}^{(j)} \quad (4)$$

By applying eq. (1) eventually both the centrifugal and Coriolis induced forces and torques respectively can be determined.

$$c(q, \dot{q}) = C \cdot \dot{q} \quad (5)$$

Thus, the dynamic equation of the robot is

$$\mathbf{M}(\mathbf{q})\ddot{\mathbf{q}} + \mathbf{c}(\mathbf{q}, \dot{\mathbf{q}}) + \mathbf{g}(\mathbf{q}) = \boldsymbol{\tau}. \quad (6)$$

3.2. Flexible joint model for a hybrid drive robot

In contrast to the idealized rigid body model above the real robot features limited gear box stiffness, friction, backlash, etc. These effects can be appended via additional matrices. Gear box stiffness usually is represented by a torsional spring. Assuming that kinetic energy only results from a rotation about the respective motor drive axis the corresponding torques are calculated by

$$\boldsymbol{\tau}_{\text{spring}} = \mathbf{K}_E \cdot (\mathbf{q}_M - \mathbf{q}) \text{ with } \mathbf{K}_E = \begin{pmatrix} -\mathbf{K} & \mathbf{K} \\ \mathbf{K} & -\mathbf{K} \end{pmatrix}. \quad (7)$$

\mathbf{K} is a diagonal matrix with the torsional stiffness of the gear box of each joint drive. Thus, the dynamic system has to be expanded by the generalized variables \mathbf{q}_M representing the drive-sided motor angles. \mathbf{q} and \mathbf{q}_M are generally different by reason of limited joint stiffness and backlash. Furthermore the drive motors represent an additional dynamic system that has to be considered (cf. eq. (8)). Eventually the mechanical model of the robot follows eq. (9).

$$\mathbf{J}_M \ddot{\mathbf{q}}_M + \mathbf{K}(\mathbf{q}_M - \mathbf{q}) + \mathbf{F}_{vSM} \dot{\mathbf{q}}_M + \dots \quad (8)$$

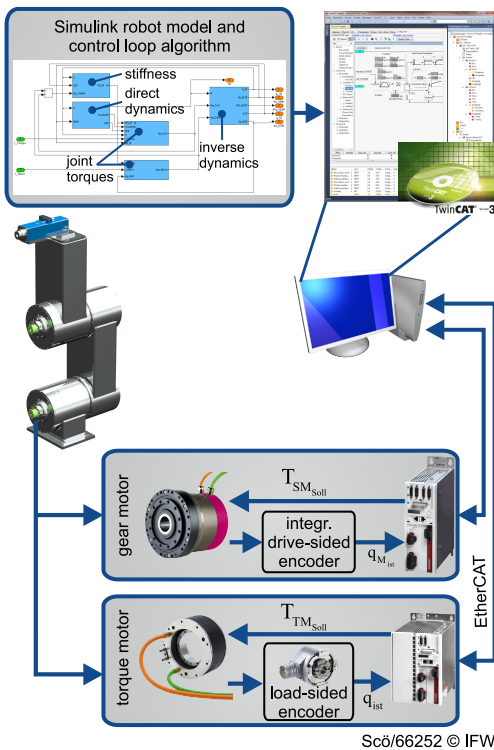


Fig. 2: Real-time control environment

$$\mathbf{F}_{S_{SM}} \text{sign}(\mathbf{q}_M) = \boldsymbol{\tau}_{SM}$$

$$\begin{aligned} & \left(\begin{matrix} \mathbf{M}(\mathbf{q}) & \mathbf{0} \\ \mathbf{0} & \mathbf{J}_M \end{matrix} \right) \left(\begin{matrix} \ddot{\mathbf{q}} \\ \dot{\mathbf{q}}_M \end{matrix} \right) + \mathbf{C}(\mathbf{q}) \left(\begin{matrix} \dot{\mathbf{q}} \\ \mathbf{0} \end{matrix} \right) + \dots \\ & \left(\begin{matrix} \mathbf{F}_v \\ \mathbf{F}_{vSM} \end{matrix} \right) \left(\begin{matrix} \dot{\mathbf{q}} \\ \dot{\mathbf{q}}_M \end{matrix} \right) + \mathbf{K}_E \left(\begin{matrix} \mathbf{q} \\ \mathbf{q}_M \end{matrix} \right) + \mathbf{g}(\mathbf{q}) + \dots \\ & \left(\begin{matrix} \mathbf{F}_S \\ \mathbf{F}_{S_{SM}} \end{matrix} \right) \left(\begin{matrix} \text{sign}(\mathbf{q}) \\ \text{sign}(\mathbf{q}_M) \end{matrix} \right) = \left(\begin{matrix} \boldsymbol{\tau}_{TM} + \boldsymbol{\tau}_{ext} \\ \boldsymbol{\tau}_{SM} \end{matrix} \right) \end{aligned} \quad (9)$$

In this formulation \mathbf{J}_M represents the inertia and $\boldsymbol{\tau}_{SM}$ the motor torques of the drive-sided servo gear motors. $\boldsymbol{\tau}_{TM}$ is the vector of the torques of the load-sided applied torque motors while $\boldsymbol{\tau}_{ext}$ represents the vector of the torques affecting the joints due to external loads, e.g. process forces. Furthermore the equations are extended with viscous and static friction both on the drive (\mathbf{F}_{vSM} , $\mathbf{F}_{S_{SM}}$) and the load side (\mathbf{F}_v , \mathbf{F}_S). However, as a result of the gear ratio the influence of the drive-sided friction effect is generally considerably higher.

For designing the control algorithms a state space model is required. Using the state vector $\mathbf{x} = (\mathbf{q} \ \dot{\mathbf{q}} \ \mathbf{q}_M \ \dot{\mathbf{q}}_M)^T$ and the input vector $\mathbf{u} = (\boldsymbol{\tau}_{TM} \ \boldsymbol{\tau}_{SM})^T$ the dynamic behavior of the robot can be represented by the following state space matrices. In this state space model the nonlinear terms $\mathbf{c}(\mathbf{q}, \dot{\mathbf{q}})$ and $\mathbf{g}(\mathbf{q})$ are neglected. In the control concept they are separately handled (cf. chapter 4.2).

$$\mathbf{A} = \begin{pmatrix} \mathbf{0} & \mathbf{1} & \mathbf{0} & \mathbf{0} \\ -\mathbf{M}^{-1}\mathbf{K} & -\mathbf{M}^{-1}\mathbf{F}_S & \mathbf{M}^{-1}\mathbf{K} & \mathbf{M}^{-1}\mathbf{F}_{S_{SM}} \\ \mathbf{0} & \mathbf{0} & \mathbf{0} & \mathbf{1} \\ \mathbf{J}_M^{-1}\mathbf{K} & \mathbf{J}_M^{-1}\mathbf{F}_S & -\mathbf{J}_M^{-1}\mathbf{K} & -\mathbf{J}_M^{-1}\mathbf{F}_{S_{SM}} \end{pmatrix} \quad (10)$$

$$\mathbf{B} = \begin{pmatrix} \mathbf{0} & \mathbf{0} \\ \mathbf{M}^{-1} & \mathbf{0} \\ \mathbf{0} & \mathbf{0} \\ \mathbf{0} & \mathbf{J}_M^{-1} \end{pmatrix} \quad (11)$$

$$\mathbf{C} = \begin{pmatrix} \mathbf{1} & \mathbf{0} & \mathbf{0} & \mathbf{0} \\ \mathbf{0} & \mathbf{0} & \mathbf{1} & \mathbf{0} \end{pmatrix} \quad (12)$$

4. Control of the Hybrid Drives

4.1. Real time control

Based on the previously presented flexible joint robot model a closed loop control is designed. The demand for a highly dynamic compensation of angle errors and thus end-effector position deviations requires a real time capable control environment. To gather respective measured values in real time the application of the EtherCAT bus is aspired because synchronized cycle times up to 12.5 µs are obtainable. Moreover, the usage of Beckhoff's TwinCAT control technology enables to directly implement Matlab Simulink models and control loop algorithms. Thereby a real time computation of the robots nonlinear system behavior is possible. Furthermore, this provides the integration of adaptive

control loop strategies using control loops that are adjusted and optimized online. An overview of the pursued control scenario is shown in Fig. 2. The angular measurement information of both the load-sided applied servo gear motor encoder and the drive-sided utilized torque motor encoder are transmitted to the control PC via EtherCAT. The TwinCAT-integrated controller computes online the inverse dynamics and thus the inertia matrix, centrifugal and Coriolis as well as gravity-related torques. Eventually set values for the respective motor torques are calculated and transmitted to the motor converter.

4.2. Model-based feedback control

The control algorithm is based on the state space model of eqn. (10) to (12). It relies on a preferably well linearization of the nonlinear robot behavior. Therefore, the nonlinear parts, consisting of gravity and centrifugal and Coriolis terms are to be pilot controlled (cf. Fig. 3). To obtain optimal quality of control and high robustness at once here a combination of an adaptive state controller and a PI multi value controller is chosen. For designing the adaptive state controller a LQR is applied. For a system of eqn. (13) and (14) with the controller of eq. (15)

$$\dot{\mathbf{x}}(t) = \mathbf{A}\mathbf{x}(t) + \mathbf{B}\mathbf{u}(t) \quad (13)$$

$$\mathbf{y}(t) = \mathbf{C}\mathbf{x}(t) \quad (14)$$

$$\mathbf{u}(t) = -\mathbf{K}_R \mathbf{x}(t) \quad (15)$$

the resulting system is controlled optimally when the control matrix \mathbf{K}_R follows

$$\mathbf{K}_R = \mathbf{R}^{-1} \mathbf{B}^T \mathbf{P}. \quad (16)$$

In this context \mathbf{P} is the symmetric, positive definite solution of the Matrix-Riccati-Equation [13]. \mathbf{R} and \mathbf{Q} represent weighting matrices. According to [14] \mathbf{R} corresponds to the control energy which is equivalent to weighting the actuating variables and with \mathbf{Q} the systems state variables are weighted.

In the considered context system matrix \mathbf{A} is varying because of $\mathbf{M}(\mathbf{q})$ (eq. (10)). Since \mathbf{P} depends on \mathbf{A} , \mathbf{K}_R has to be recalculated for every time step.

However, an optimal quality of control depends on the weighting matrices \mathbf{R} and \mathbf{Q} . The dimension of those is a consequence of the systems number of states and thus determines the degrees of freedom for selecting \mathbf{Q} and \mathbf{R} . In the context of the above presented robot model with hybrid drives each motor type is controlled with a separate state controller. For each motor type \mathbf{Q} has 8x8- and \mathbf{R} 2x2-dimension. With respect to [15] diagonal matrices for \mathbf{Q} and \mathbf{R} are selected which results in 20 degrees of freedom for the state controller design. Due to this high number of degrees of freedom a genetic

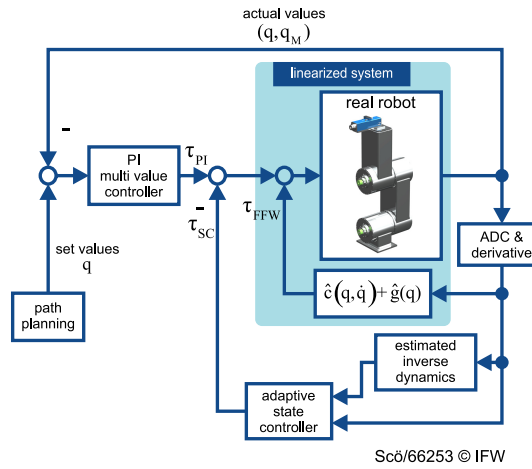


Fig. 3: Model-based feedback control

algorithm (GA) is applied to achieve optimal matrices \mathbf{R} and \mathbf{Q} . Therefore, separate state space models for each motor type are derived and the respective diagonal matrix elements of the weighting matrices are used as parameters for the GA. To evaluate the quality of control with each parameter set the step responses are examined. As fitness function a minimal settling time, an avoidance of overshoots as well as higher eigenvalues of the torque motor controlled system compared to the gear motor controlled system are chosen. The pre-cascaded PI-multi-value controller represents the pre-filter and additionally provides for compensating control deviations. Again the PI-controller are separated between the servo gear motor and the torque motor resulting in decoupled controllers.

4.3. Simulation results

To investigate and evaluate the hybrid drive concept with its model-based control approach the above presented model was used for simulation. In addition to joint compliance and friction a machining process force model was implemented. It emulates a high speed cutting process of aluminum and affects the robot via disturbances in each joint. The peak torque in joint one is approximately 250 Nm. In the simulation an angle step of $\mathbf{q} = [-1.5708 \ 0] \rightarrow [0 \ 0]$ was realized to evaluate settling times, accuracies and compensation of induced angle errors. Here q_1 and q_2 correspond to the joint angles of axis 1 and 2 respectively. In the comparison scenario the chosen torque motor merely provides approximately 15% of the total joint torque.

In Fig.4(a) depicts that the application of an additional torque motor results in lower overshoots and lower settling times compared to the case with only one servo gear motor. Moreover, in the detailed view of Fig.4(b) it is shown, that amplitudes of the angle error can be decreased by factor 8 (joint 1) and 25 (joint 2)

respectively. Thus, both the positioning dynamic and the compensation of angle errors are achievable even with a small torque ratio between torque and servo motor. However the applied control approach has still to be optimized to compensate the control deviation, which amongst other things currently is caused by missing anti-windup-reset structures for the integrators.

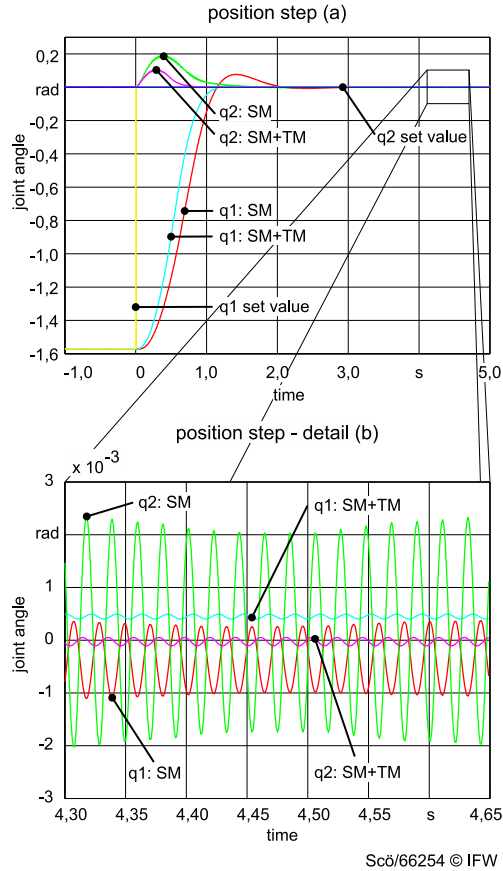


Fig.4: Step-response of joint angles for servo motor controlled (SM) and servo and torque motor controlled (SM+TM) robot

5. Conclusion

In this paper an innovative hybrid drive concept for robots is introduced. It features a parallel connection of both servo gear motor and torque motor as well as drive-sided and load-sided encoders. The simulation results show a considerable better control behavior when applying the torque motor, especially concerning the compensation of dynamic deviations. Regarding the aspired application range of machining better results are anticipated. That qualifies robots with this drive concept for much more sophisticated machining tasks than state of the art robots are being applied for.

In future researches the design components will be analyzed using finite element to optimize it regarding weight and stiffness. Subsequently the test bed will be

assembled to identify stiffness, friction and mass parameters necessary for modeling the real robot and optimizing the control for it. Moreover, the corresponding control hardware, e.g. converters and controller, will be set up to verify the simulations.

Acknowledgements

The authors would like to thank the ministry of science and culture of Lower Saxony (MWK) for funding the research project within the cluster “Pro³gression” (www.pro3gression.uni-hannover.de).

References

- [1] Hu, Y. N.; Chen, Y. H.: Implementation of a Robot System for Sculptured Surface Cutting. Part 1. Rough Machining. *The International Journal of Advanced Manufacturing Technology*, Vol. 9: Nr. 15, S. 624–629, 1999.
- [2] Pan Z, Zhang H: Improving robotic machining accuracy by real-time compensation. ICROS-SICE Inter. Joint Conference, Fukuoka, Japan, S. 4289–4294, 2009.
- [3] Bauer, J.; Friedmann, M.; Hemker, T.; Pischan, M.; Reinl, C.; Abele, E.; Stryk, O.: Analysis of Industrial Robot Structure and Milling Process Interaction for Path Manipulation. In: Berend Denkena und Ferdinand Hollmann (Hg.): *Process Machine Interactions*: Springer Berlin Heidelberg (Lecture Notes in Production Engineering), pp. 245–263, 2013.
- [4] Abele, E.; Bauer, J.; Rothenbücher, S.; Stelzer, M.; Stryk, O.: Prediction of the Tool Displacement by Coupled Models of the Compliant Industrial Robot and the Milling Process. Conference on Process Machine Interaction, Hannover, 2008
- [5] Abele, E.; Schützer, K.; Bauer, J.; Pischan, M.: Tool path adaption based on optical measurement data for milling with industrial robots. In: *Production Engineering* 6 (4-5), pp. 459–465, 2012.
- [6] Abele, E., Weigold, M., Rothenbücher, S.: Modeling and Identification of an Industrial Robot for Manufacturing Applications. In: *CIRP Annals - Manufacturing Technology*, Vol. 56, Nr. 1, pp. 387-390, 2007.
- [7] Chen, Yonghua; Dong, Genghua: Robot machining: recent development and future research issues, *International Journal of Advanced Manufacturing Technology*, pp. 1-9, 2012.
- [8] Chunhe G.; Jingxia Yuan; J. N.: Nongeometric error identification and compensation for robotic system by inverse calibration. In: *International Journal of Machine Tools and Manufacture* 40 (14), pp. 2119–2137, 2000.
- [9] Feng-yun, L.; Tian-sheng, L.: Development of a robot system for complex surfaces polishing based on CL data. In: *The International Journal of Advanced Manufacturing Technology* 26 (9-10), pp. 1132–1137, 2005.
- [10] Asada, H.; Youcef-Toumi, K.: *Direct-drive robots: theory and practice*. Mit Pr, 1987.
- [11] Reyes, F.; Kelly, R.: Experimental Evaluation of Identification Schemes on a Direct Drive Robot. *Robotica*, Vol. 05, Nr. 15, S. 563–571, 1997.
- [12] Siciliano, B.; Sciavicco, L.; Villani, L.; Oriolo, G.: *Robotics: Modelling, Planning and Control*. Advanced Textbooks in Control and Signal Processing. Springer Verlag, 2009.
- [13] Agrawal, A. K.; Yang, J. N.: Design of Passive Energy Dissipation Systems Based on LQR Control Methods. *Journal of Intelligent Material Systems and Structure* 12(10):933–944, 1999.
- [14] Glover, K.; Doyle, J.; Zhou, K.: *Robust and Optimal Control*: Prentice Hall, 1995.
- [15] Molinari, B.: Redundancy in linear optimum regulator problem. In: *Automatic Control, IEEE Transactions on* 16 (1), pp. 83–85, 1971.